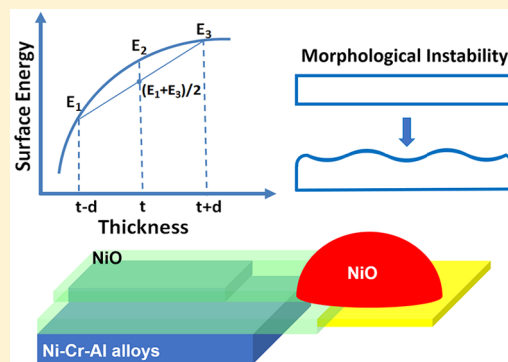# Direct Observation of "Pac-Man" Coarsening

X. X. Yu,*[†] A. Gulec,[†] A. Yoon,[‡] J. M. Zuo,[‡] P. W. Voorhees,[†] and L. D. Marks[†]

[†]Department of Materials Science and Engineering, Northwestern University, Evanston, Illinois 60208, United States
[‡]Department of Materials Science and Engineering, University of Illinois, Urbana-Champaign, Illinois 61801, United States

Ⓢ Supporting Information

ABSTRACT: We report direct observation of a "Pac-Man" like coarsening mechanism of a self-supporting thin film of nickel oxide. The ultrathin film has an intrinsic morphological instability due to surface stress leading to the development of local thicker regions at step edges. Density functional theory calculations and continuum modeling of the elastic instability support the model for the process.

KEYWORDS: Oxide, thin film, coarsening, in situ, environmental TEM

Ni-based superalloys have been widely used for the high temperature applications due to their excellent mechanical properties and oxidation resistance.[1,2] The typical microstructure of these alloys involves a γ'-Ni_3Al phase with a $L1_2$ structure coherently embedded in a solid solution matrix of the γ-Ni phase.[3] Alloying elements, such as Cr, are added to enhance the high-temperature oxidation resistance.[4] Prior studies show that the general oxidation mechanism depends on the composition and the temperature, and the formation of a continuous film of Cr_2O_3 or Al_2O_3 in Ni−Cr−Al alloys significantly decreases further oxidation of the alloy.[5] Although comprehensive oxidation research[6−8] has been conducted on steady state oxidation where the oxides fully developed to thermodynamically stable scales, the early oxidation stages are not well-understood. These usually includes oxide nucleation, island growth and then the formation of a continuous oxide layer. Although a few in situ transmission electron microscopy (TEM) studies have been carried out for Ni−Cr and Ni−Al alloy oxidation,[9−13] the evolution of the oxide thin film and the growth kinetics are relatively unknown.

Moving beyond these alloys, the stability and evolution of thin films is an important issue in the area of microelectronic device, catalysis, and oxidation.[14,15] A bounded thin film on a substrate is subject to capillary instability at the ends of the film and will tend to change its morphology to reduce surface energy through mass transfer by diffusion.[16] It has been observed in many different systems that an initially straight edge of the thin film can be unstable and develop large amplitude undulations and retract with a constant speed.[17−19] Several thermodynamic models have been proposed based on capillarity-driven surface diffusion, and numerical simulations have been performed to illuminate the experimental observa-

tions.[20−22] In addition, it is possible for the stress generated by the mismatch in lattice parameter between the film and the substrate to lead to a morphological instability of a planar film. In this case the instability is driven by the reduction in bulk elastic energy of the film and substrate.

However, the above are for thin films on a substrate, not for a free-standing thin film. While such a thin film is obviously unstable with respect to a surface-energy driven instability at the ends of the film, we find here an instability that is driven by the elastic energy that results from the surface stress. In this Letter, we demonstrate this both experimentally using in situ TEM coupled with density functional theory (DFT) calculations and a linear stability analysis. The instability begins at step edges and leads to a nonlinear instability reminiscent of a "Pac-Man" like coarsening mechanism where thicker regions form at step edges that then retract toward the thicker portion of the film, in effect "eating" a layer out of the thin film. These locally thicker regions resemble nanoparticles of one material on a substrate composed of a different material but are instead locally thicker regions of the material oxide on a thin film of the same material (here nickel oxide).

Ternary $Ni_{67.5}Cr_{22.5}Al_{10}$ (at. %) alloys were arc-melted and copper mold suction cast. Heat treatments were carried out in a tube furnace in the ambient air at 1330 °C for 20 h followed by a water quench. The annealing eliminates the solidification microstructure and chemical segregation forming a uniform grain size (on the micron scale) and homogeneous element distribution. The sample was then polished using diamond
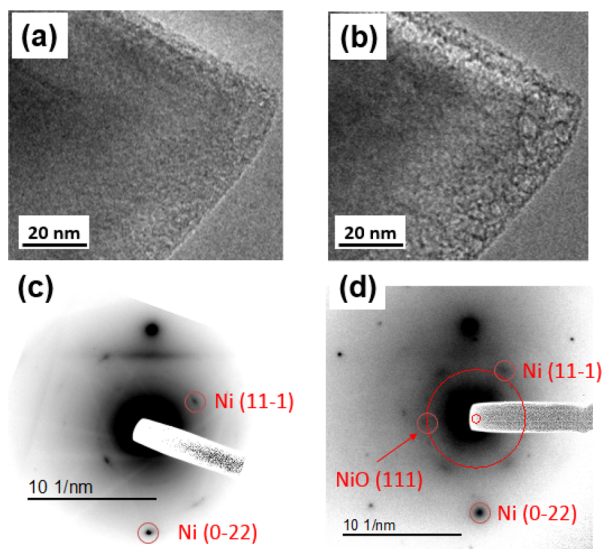
lapping paper, and the powders were collected and attached to the tungsten wire by a clean brush. In situ oxidation experiments were carried using a Hitachi H-9500 ETEM with a LaB_6 emitter at UIUC operated at 300 kV.[23] A special holder designed for the ETEM provides a gas injection and heating environment directly on the sample. After heating the $Ni_{67.5}Cr_{22.5}Al_{10}$ sample above 800 °C at the base pressure of 9×10^{-5} Pa to equilibrate the surface, we injected O_2 into the TEM to a pressure of 2×10^{-3} Pa at different temperatures.

The surface stress and the effect of strain on Ni oxide were calculated by density functional theory (DFT) calculations using the Vienna ab initio Simulation Package[24,25] with a plane wave cutoff of 550 eV. We built 6−10 NiO (100) slab models with a 15 Å vacuum region. For all of the calculations, we used the projector augmented wave method[26,27] and evaluated the exchange-correlation energy using the Purdew−Burke−Ernzerhoff[28] functional within the spin-polarized generalized gradient approximation plus Hubbard U correction following the approach of Dudarev et al.[29] Based upon calibration calculations, a value of U_{eff} = 5.3 eV for the correlated Ni 3d orbitals was used in all simulations leading to reasonable values for the band gap, formation energies, magnetic moment, and elastic constants (see Supporting Information). A $15 \times 15 \times 1$ k-mesh was used for the k points sampling using the Monkhorst−Pack[30] scheme during structural relaxation until the forces on each ion were less than 0.01 eV/Å.

The surface of the Ni−Cr−Al alloys gradually became faceted by forming NiO during low temperature oxidation (∼200 °C) for 30 min as seen in Figure 1. The diffraction
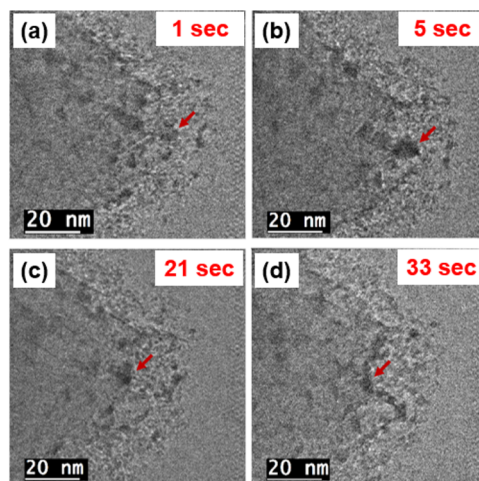

Figure 1. (a and b) Images of $Ni_{67.5}Cr_{22.5}Al_{10}$ alloy before and during oxidation and (c and d) diffraction patterns before and during oxidation.

pattern in Figure 1d during oxidation shows extra NiO (111) spots in addition to the main fcc alloy. From other studies (not shown here) the NiO was forming with a cube−cube epitaxy on the underlying metal, similar to the established epitaxy of NiO on Ni. We will only describe here results when the NiO film was free-standing and the underlying metal was not present. For completeness, under these lower temperature conditions only NiO is formed with minimal formation of spinel or other oxides at least in the initial stages of the oxidation. The growth

details are not important for this work and will be described more elsewhere.

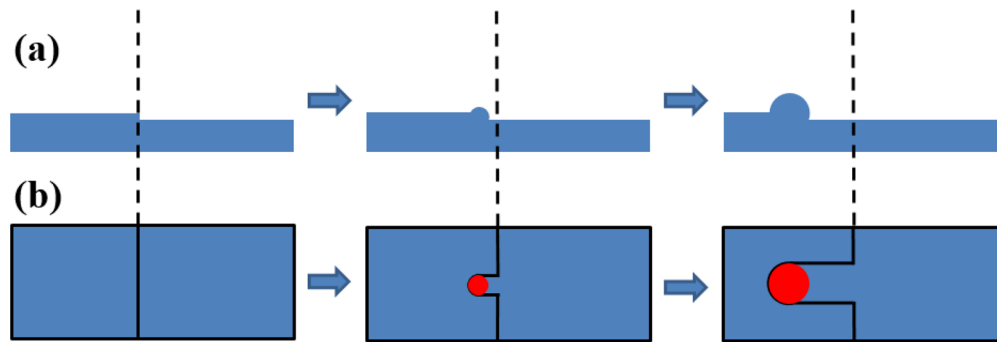When the temperature was increased to 800 °C, thicker regions of NiO on the NiO substrate formed, Figure 2b, and

Figure 2. "Pac-Man" coarsening of the NiO film with images from a time sequence (see the Supplemental Video 1 for the full process). (a) Initial step edges (red arrow). (b) The step edges thickened after 5 s. (c) Thickened edges retracted toward the thicker region of the film after 21 s. (d) Thicker regions at the step edges "eat" into the film.

then started to eat into the thin film, Figure 2c−d and Supplemental Video 1. Similar results were obtained a number of times, see Supplemental Figure S2 and Video 2 for another example.

The analysis of single frames from the videos indicated that the formation of the thicker regions was triggered by an instability at either monatomic steps or multiple height step bunches. As illustrated in Figure 3, locally the step edge thickens, retracting toward the thicker region of the film; this is not so clear in Video 1, clearer in Video 2. As the process continues, the thicker region eats into the material similar to a "Pac-Man", dragging the step with it (see Video 1 and 2). The net result is an increase in the local thickness and a thinner region of NiO left behind. The global driving force for the process is the surface stress at the surface of the oxide which will reduce the free energy of the system. However, the mechanism is different from those currently in the literature.[14,15,17,21] What we have is a morphological instability which is reminiscent of classic Rayleigh instabilities and instabilities of misfit thin films on substrates and indicates a concave total energy versus NiO film thickness for a film of constant thickness.

One possibility would be a thickness-dependent surface free energy. It is simple to show that the long-range strain associated with a surface reconstruction when truncated for a finite thickness will lead to a net reduction in energy with thickness. However, since from St. Venant's principle these strains decay into the material with a wavelength that scales as the reconstruction size (e.g., ref 31) and no large reconstructions are known for NiO, this is unlikely. Electrostatic coupling of atomic displacements (polarization changes) at the top and bottom surface are also unlikely as we expect these to be repulsive due to the pseudomirror symmetry.

A potential driving force for a surface instability is surface stress. It is well-established that this leads to a size-dependent

Figure 3. Schematic of the "Pac-Man" coarsening of NiO thin film: (a) side view; (b) top view.

change in the lattice parameters of nanoparticles from a balance of reduction in the total surface energy via a contraction or expansion and an increase in the total energy via strain.[32−34] The same process will occur for a free-standing thin film. Since the film is free-standing, the surface stress, f, imparts a force along the planar surface of the film. Assuming elastic isotropy the total energy E per unit area of a flat film of thickness l, is,

$$E = E_e + E_g = \frac{-2f^2(1 - v)}{l\mu(1 + v)}; \qquad E_e = -1/2E_g \qquad (1)$$

where μ is the shear modulus, v is Poisson's ratio, E_e is the elastic energy, and E_g is the energy associated with straining the surface, that is, the surface stress contribution. This energy diverges as $1/l$, where l is the thickness of the film. To cross-validate this form, we calculated the surface stress using DFT with anisotropic elasticity for a NiO (001) film; the results confirm this continuum formulation as shown in more detail in the Supporting Information.

While this implies that an instability can occur, it does not unconditionally prove the existence of one. For this we need to consider the possibility that this surface stress drives a surface diffusion mediated linear morphological instability of the top surface of the film. Specifically, locating the origin of the coordinate system at the unperturbed planar film, $z = 0$, the top surface of the film is perturbed by a plastic deformation (i.e., thickness change) according to,

$$z = h(x, y, t) = \hat{h}e^{\sigma t + ikx + iky} \qquad (2)$$

where for simplicity we have assumed that the wavenumber k is the same in the x and y directions, σ is the growth rate of the instability, t is time, and $\hat{h} \ll 1$. The bottom surface of the film, at $z = -l$, remains planar. The objective is to determine $\sigma(k)$; if $\sigma > 0$ then the top surface will be unstable. The surface evolves by elastic stress driven surface diffusion,[35]

$$\frac{\partial h}{\partial t} = D(1 + |\nabla h|^2)^{1/2}\nabla_s^2(W_e + \gamma\kappa) \qquad (3)$$
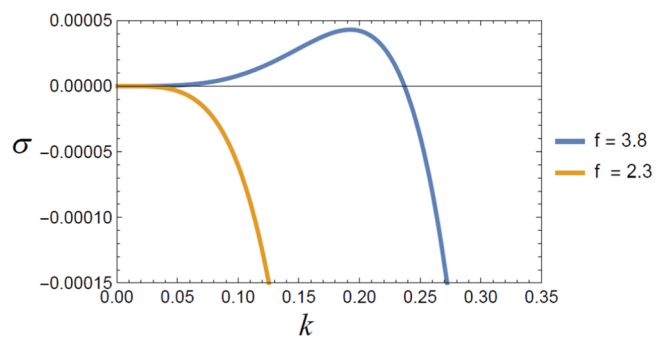
where D is a relative surface diffusion coefficient, ∇_s^2 is surface Laplacian, W_e is the elastic energy density at the surface of the film, γ is the isotropic surface energy, and κ is twice the mean curvature of the surface. In writing eq 3, we have omitted terms in the chemical potential that explicitly involve the surface stress energy change with the elastic deformation; as formulated using periodic plastic deformation, the average change in strain at the surface is zero so these terms vanish. We are also neglecting the role of the surface step (or step bunch) which experimentally is the nucleation site, and also atomistic energy terms such as step energies. Following ref 36, linearizing the

evolution equation and the stress-free boundary conditions on the top surface to first order in $\hat{h}$ solving the elasticity problem to determine the perturbed elastic energy yields the following equation for the growth rate of the instability,

$$\sigma = \left(\frac{2k^3f^2(1 - v^2)\sinh(\sqrt{2}\,k)^2}{\gamma l\mu(2v - 1)(4kl + \sqrt{2}\,(2v - 3)\sinh(2\sqrt{2}\,k))} - k^4\right) \qquad (4)$$

where σ is the dimensionless growth rate defined as $\sigma^*l^4/D\gamma$, σ^* is the dimensional growth rate, and k is the dimensionless wavenumber scaled on the thickness of the film.

To illustrate the general idea, if we choose $v = 0.4$, $\mu = 9.2 \times \frac{10^{10}J}{m^3}$, $\gamma = \frac{1.01J}{m^2}$, $l = 2.0$ nm, and $f = 2.3$ and 3.8 J/m^2; these parameter values follow from the DFT calculation, except that we chose both the DFT surface stress and one which is 50% higher as will be discussed below. The growth rate of the instability is shown in Figure 4. This shows that the surface

Figure 4. Dimensionless growth rate of the instability as a function of the dimensionless wavenumber of a fluctuation.

stress can generate an instability since $\sigma > 0$ for a range of wavelengths with the larger surface stress. For large wavenumbers, $\sigma > 0$ due to the presence of surface energy. For the DFT parameters a thin film by itself would be stable, but with a slightly higher surface stress it would not be. Experimentally we did not observe spontaneous nucleation of "Pac-Man" like thicker regions in flat regions, only nucleating at existing steps which is consistent with the analytical results. The thickness of the film has two effects on the instability. First, the stress in the film increases as $1/l$, and thus the driving force for the instability increases with decreasing film thickness. Second the planar interface on the bottom of the film acts to stabilize the film for very thin films and, in fact, can cancel the destabilizing effects of the stress generated by the surface stress in the limit that the film thickness goes to zero. Thus, the film thickness

needed to demonstrate instability in this model is a coarse approximation of what would happen in a real system.

The analytical model is in quite good agreement with the experiment, given that contains many assumptions and approximations. In the analytical model we have assumed that the bottom surface remains planar and does not evolve due to the stress generated by the perturbed top surface which may not be correct. We have also approximated by using isotropic elasticity, since the anisotropic formulation even for a simple cubic material such as NiO is much more complicated to solve. The connection between the analytical model and DFT is not perfect; for instance we have used a curvature regularization term instead of a (more accurate) step or vicinal surface formulation. The DFT numbers are not themselves without possible error, and the surface free energy and surface stress are probably underestimates. On top of these, it is well-established that chemisorption can substantially change surface free energies and surface stresses. Furthermore, accurate models that allow for morphological changes on the top and bottom surfaces, as well as a full representation of the effects of the surface stress on chemical potential, are needed to make this model quantitative. Most importantly, the model shows that as a result of a nonzero surface stress a film will be unstable to perturbations in the morphology of the top surface, which the presence of a step on the surface provides as a nucleation site.

In summary, we have found a new instability for a self-supporting thin film where the driving force is the reduction in the energy due to surface stress, which is different from the drivers for other types of instabilities in the literature. We believe that there may be many other cases where similar "Pac-Man" like instabilities occur.

■ ASSOCIATED CONTENT

Ⓢ Supporting Information

The Supporting Information is available free of charge on the ACS Publications website at DOI: 10.1021/acs.nano-lett.7b01137.

> Additional images and diffraction of the initial NiO; images from a second video of the time evolution, density functional calculations to confirm the role of surface stress (PDF)

> Time evolution of the formation of thicker regions of NiO on the NiO substrate (AVI)

> Time evolution of the formation of thicker regions of NiO on the NiO substrate, showing clearer retraction of step edge (AVI)

■ AUTHOR INFORMATION

ORCID Ⓘ

X. X. Yu: 0000-0001-7322-2577

Notes

The authors declare no competing financial interest.

■ ACKNOWLEDGMENTS

■ REFERENCES

(1) Caron, P.; Khan, T. *Aerosp. Sci. Technol.* **1999**, *3* (8), 513−523.

(2) Reed, R. C. *The superalloys: fundamentals and applications*; Cambridge University Press, 2008.

(3) Pollock, T. M.; Tin, S. *J. Propul. Power* **2006**, *22* (2), 361−374.

(4) Giggins, C.; Pettit, F. *J. Electrochem. Soc.* **1971**, *118* (11), 1782−1790.

(5) Hindam, H.; Whittle, D. *Oxid. Met.* **1982**, *18* (5−6), 245−284.

(6) Hou, P.; Stringer, J. *Oxid. Met.* **1990**, *34* (3−4), 299−321.

(7) Kear, B.; Pettit, F.; Fornwalt, D.; Lemaire, L. *Oxid. Met.* **1971**, *3* (6), 557−569.

(8) Douglass, D. *Corros. Sci.* **1968**, *8* (9), 665−678.

(9) Luo, L.; Zou, L.; Schreiber, D. K.; Olszta, M. J.; Baer, D. R.; Bruemmer, S. M.; Zhou, G.; Wang, C.-M. *Chem. Commun.* **2016**, *52* (16), 3300−3303.

(10) Luo, L.; Zou, L.; Schreiber, D. K.; Baer, D. R.; Bruemmer, S. M.; Zhou, G.; Wang, C.-M. *Scr. Mater.* **2016**, *114*, 129−132.

(11) Qin, H.; Chen, X.; Li, L.; Sutter, P. W.; Zhou, G. *Proc. Natl. Acad. Sci. U. S. A.* **2015**, *112* (2), E103−E109.

(12) Wang, C.-M.; Schreiber, D. K.; Olszta, M. J.; Baer, D. R.; Bruemmer, S. M. *ACS Appl. Mater. Interfaces* **2015**, *7* (31), 17272−17277.

(13) Wang, C.-M.; Genc, A.; Cheng, H.; Pullan, L.; Baer, D. R.; Bruemmer, S. M. *Sci. Rep.* **2015**, *4*, 03683.

(14) Jiran, E.; Thompson, C. *Thin Solid Films* **1992**, *208* (1), 23−28.

(15) Thompson, C. V. *Annu. Rev. Mater. Res.* **2012**, *42*, 399−434.

(16) Balluffi, R. W.; Allen, S.; Carter, W. C. *Kinetics of materials*; John Wiley & Sons, 2005.

(17) Kim, G. H.; Zucker, R. V.; Ye, J.; Carter, W. C.; Thompson, C. V. *J. Appl. Phys.* **2013**, *113* (4), 043512.

(18) Srolovitz, D.; Safran, S. *J. Appl. Phys.* **1986**, *60* (1), 255−260.

(19) Zucker, R. V. *Capillary-driven shape evolution in solid-state micro- and nano-scale systems*l Massachusetts Institute of Technology, 2015.

(20) McCallum, M. S.; Voorhees, P. W.; Miksis, M. J.; Davis, S. H.; Wong, H. *J. Appl. Phys.* **1996**, *79* (10), 7604−7611.

(21) Wong, H.; Miksis, M. J.; Voorhees, P. W.; Davis, S. H. *Acta Mater.* **1997**, *45* (6), 2477−2484.

(22) Wong, H.; Voorhees, P.; Miksis, M.; Davis, S. *Acta Mater.* **2000**, *48* (8), 1719−1728.

(23) Yoon, A.; Zhang, X.; Gao, W.; Wu, J.; Pan, Y.-T.; Yang, H.; Zuo, J.-M. *Microsc. Microanal.* **2014**, *20* (S3), 1864−1865.

(24) Kresse, G.; Hafner, J. *Phys. Rev. B: Condens. Matter Mater. Phys.* **1993**, *47* (1), 558.

(25) Kresse, G.; Furthmüller, J. *Phys. Rev. B: Condens. Matter Mater. Phys.* **1996**, *54* (16), 11169−11186.

(26) Blöchl, P. E. *Phys. Rev. B: Condens. Matter Mater. Phys.* **1994**, *50* (24), 17953.

(27) Kresse, G.; Joubert, D. *Phys. Rev. B: Condens. Matter Mater. Phys.* **1999**, *59* (3), 1758.

(28) Perdew, J. P.; Burke, K.; Ernzerhof, M. *Phys. Rev. Lett.* **1996**, *77* (18), 3865.

(29) Dudarev, S.; Botton, G.; Savrasov, S.; Humphreys, C.; Sutton, A. *Phys. Rev. B: Condens. Matter Mater. Phys.* **1998**, *57* (3), 1505.

(30) Monkhorst, H. J.; Pack, J. D. *Phys. Rev. B* **1976**, *13* (12), 5188.

(31) Marks, L. D.; Xu, P.; Dunn, D. N. *Surf. Sci.* **1993**, *294* (3), 322−332.

(32) Marks, L. *Rep. Prog. Phys.* **1994**, *57* (6), 603.

(33) Dingreville, R.; Qu, J.; Cherkaoui, M. *J. Mech. Phys. Solids* **2005**, *53* (8), 1827−1854.

(34) Marks, L.; Peng, L. *J. Phys.: Condens. Matter* **2016**, *28* (5), 053001.

(35) Spencer, B.; Voorhees, P.; Davis, S. *Phys. Rev. Lett.* **1991**, *67* (26), 3696.

(36) Spencer, B.; Voorhees, P.; Davis, S. *J. Appl. Phys.* **1993**, *73* (10), 4955−4970.